Kim VN (2005) MicroRNA biogenesis: coordinated cropping and dicing. *Nature Rev Mol Cell Biol* **6**: 376-385.

Laemmli UK (1970) Cleavage of structural proteins during the assembly of the head of bacteriophage T4. *Nature* **227**: 680-685.

Lechner D, Manhardt T, Bajna E, Posner GH and Cross HS (2006) A 24-phenylsulfone analog of vitamin D inhibits 1α,25-dihydroxyvitamin D_3 degradation in vitamin D metabolism-competent cells. *J Pharmacol Exp Ther* (In Press)

Lee RC, Feinbaum RL and Ambros V (1993) The *C. elegans* heterochronic gene *lin-4* encodes small RNAs with antisense complementarity to *lin-14*. *Cell* **75**: 843-854.

Lee Y, Ahn C, Han J, Choi H, Kim J, Yim J, Lee J, Provost P, Radmark O, Kim S and Kim VN (2003) The nuclear RNase III Drosha initiates microRNA processing. *Nature* **425**: 415-419.

Lewis BP, Burge CB and Bartel DP (2005) Conserved seed pairing, often flanked by adenosines, indicates that thousands of human genes are microRNA targets. *Cell* **120**: 15-20.

Lou YR, Qiao S, Talonpoika R, Syvala H and Tuohimaa P (2004) The role of vitamin D_3 metabolism in prostate cancer. *J Steroid Biochem Mol Biol* **92**: 317-325.

Lu J, Getz G, Miska EA, Alvarez-Saavedra E, Lamb J, Peck D, Sweet-Cordero A, Ebert BL, Mak RH, Ferrando AA, Downing JR, Jacks T, Horvitz HR and Golub TR (2005) MicroRNA expression profiles classify human cancers. *Nature* **435**: 834-838.

Lund E, Guttinger S, Calado A, Dahberg JE and Kutay U (2004) Nuclear export of microRNA precursors. *Science* **303**: 95-98.

de Lyra EC, da Silva IA, Katayama ML, Brentani MM, Nonogaki S, Goes JC and Folgueira MA (2006) 25(OH)D_3 and 1,25$(OH)_2D_3$ serum concentration and breast tissue expression of 1α-hydroxylase, 24-hydroxylase and vitamin D receptor in women with and without breast cancer. *J Steroid Biochem Mol Biol* **100**: 184-192.

Meltzer PS (2005) Cancer genomics: small RNAs with big impacts. *Nature* **435**: 745-746.

Miller GJ, Stapleton GE, Hedlund TE and Moffat KA (1995) Vitamin D receptor expression, 24-hydroxylase activity, and inhibition of growth by 1α,25-dihydroxyvitamin D_3 in seven human prostatic carcinoma cell lines. *Clin Cancer Res* **1**; 997-1003.

Nagpal S, Na S and Rathnachalam R (2005) Noncalcemic actions of vitamin D receptor ligands. *Endocr Rev* **26**: 662-687.

Ohyama Y, Ozono K, Uchida M, Yoshimura M, Shinki T, Suda T and Yamamoto O (1996) Functional assessment of two vitamin D-responsive elements in the rat 25-hydroxyvitamin D_3 24-hydroxylase gene. *J Biol Chem* **271**: 30381-30385.

Ren S, Nguyen L, Wu S, Encinas C, Adams JS and Hewison M (2005) Alternative splicing of vitamin D-24-hydroxylase: a novel mechanism

for the regulation of extrarenal 1,25-dihydroxyvitamin D synthesis. *J Biol Chem* **280**: 20604-20611.

Sakaki T, Sawada N, Komai K, Shiozawa S, Yamada S, Yamamoto K, Ohyama Y and Inouye K (2000) Dual metabolic pathway of 25-hydroxyvitamin D_3 catalyzed by human CYP24. *Eur J Biochem* **267**: 6158-6165.

Segersten U, Holm PK, Bjorklund P, Hessman O, Nordgren H, Binderup L, Akerstrom G, Hellman P and Westin G (2005) 25-Hydroxyvitamin D_3 1α-hydroxylase expression in breast cancer and use of non-1α-hydroxylated vitamin D analogue. *Breast Cancer Res* **7**: R980-R986.

Sempere LF, Freemantle S, Pitha-Rowe I, Moss E, Dmitrovsky E and Ambros V (2004) Expression profiling of mammalian microRNAs uncovers a subset of brain-expressed microRNAs with possible roles in murine and human neuronal differentiation. *Genome Biol* **5**: R13.

Takamizawa J, Konishi H, Yanagisawa K, Tomida S, Osada H, Endoh H, Harano T, Yatabe Y, Nagino M, Nimura Y, Mitsudomi T and Takahashi T (2004) Reduced expression of the let-7 microRNAs in human lung cancers in association with shortened postoperative survival. *Cancer Res* **64**: 3753-3756.

Towbin H, Staehelin T and Gordon J (1979) Electrophoretic transfer of proteins from polyacrylamide gels to nitrocellulose sheets: procedure and some applications. *Proc Natl Acad Sci USA* **76**: 4350-4354.

Townsend K, Banwell CM, Guy M, Colston KW, Mansi JL, Stewart PM, Campbell MJ and Hewison M (2005a) Autocrine metabolism of vitamin D in normal and malignant breast tissue. *Clin Cancer Res* **11**: 3579-3586.

Townsend K, Evans KN, Campbell MJ, Colston KW, Adams JS and Hewison M (2005b) Biological actions of extra-renal 25-hydroxyvitamin D-1α-hydroxylase and implications for chemoprevention and treatment. *J Steroid Biochem Mol Biol* **97**: 103-109.

Tsuchiya Y, Nakajima M, Kyo S, Kanaya T, Inoue M and Yokoi T (2004) Human CYP1B1 is regulated by estradiol via estrogen receptor. *Cancer Res* **64**: 3119-3125.

Tsuchiya Y, Nakajima M, Takagi S, Taniya T and Yokoi T (2006) MicroRNA regulates the expression of human cytochrome P450 1B1. *Cancer Res* **66**: 9090-9098.

Welsh J, Wietzke JA, Zinser GM, Byrne B, Smith K and Narvaez CJ (2003) Vitamin D-3 receptor as a target for breast cancer prevention. *J Nutr* **133**: 2425S-2433S.

Wightman B, Ha I and Ruvkun G (1993) Posttranscriptional regulation of the heterochronic gene *lin-14* by *lin-4* mediates temporal pattern formation in *C. elegans*. *Cell* **75**: 855-862.

Xie X, Lu J, Kulbokas EJ, Golub TR, Mootha V, Lindblad-Toh K, Lander ES and Kellis M (2005) Systematic discovery of regulatory motifs in human promoters and 3'UTRs by comparison of several mammals. *Nature* **434**: 338-345.

Zehnder D, Bland R, Williams MC, McNinch RW, Howie AJ, Stewart PM and Hewison M (2001) Extrarenal expression of 25-hydroxyvitamin D_3-1α-hydroxylase. *J Clin Endocrinol Metab* **86**: 888-894.

Zierold C, Reinholz GG, Mings JA, Prahl JM and DeLuca HF (2000) Regulation of the porcine 1,25-dihydroxyvitamin D_3-24-hydroxylase (CYP24) by 1,25-dihydroxyvitamin D_3 and parathyroid hormone in AOK-B50 cells. *Arch Biochem Biophys* **381**: 323-327.

Zierold C, Mings JA and DeLuca HF (2001) Parathyroid hormone regulates 25-hydroxyvitamin D_3-24-hydroxylase mRNA by altering its stability. *Proc Natl Acad Sci USA* **98**: 13572-13576

III. 研究成果の刊行に関する一覧表

別紙4

研究成果の刊行に関する一覧表

雑誌

発表者氏名	論文タイトル名	発表誌名	巻号	ページ	出版年
Shingo Takagi, Miki Nakajima, Takuya Mohri, and Tsuyoshi Yokoi	Post-transcriptional regulation of human pregnane X receptor by microRNA affects the expression of cytochrome P450 3A4	Journal of Biological Chemistry	283	9674-9680	2008
Shiori Takahashi, Miki Katoh, Takashi Saitoh, Miki Nakajima and Tsuyoshi Yokoi	Allosteric kinetics of human carboxylesterase 1: species differences and interindividual variability.	Journal of Pharmaceutical Science	97	5434-5445	2008
Tatsuki Fukami, Miki Katoh, Tsuyoshi Yokoi, and Miki Nakajima	Human cytochrome P450 2A13 efficiently metabolizes chemicals in air pollutants: naphthalene, styrene, and toluene.	Chemical Research in Toxicology	21	720-725	2008
Keiichi Minami, Miki Nakajima, Yuto Fujiki, Miki Katoh, Frank J. Gonzalez, and Tsuyoshi Yokoi	Regulatiion of insulin-like growth factor binding protein-1 and lipoprotein lipase by aryl hydrocarbon receptor.	Journal of Toxicological Sciense	33	405-413	2008
Akiko Nakamura, Miki Nakajima, Hiroyuki Yamanaka, Ryoichi Fujiwara, and Tsuyoshi Yokoi	Expression of UGT1A and UGT2B mRNA in human normal tissues and various cell lines.	Drug Metabolism and Disposition	36	1461-1464	2008
Hirotada Shiratani, Miki Katoh, Miki Nakajima, and Tsuyoshi Yokoi	Species differences in UGT-glucuronosyltransferase activities in mice and rats.	Drug Metabolism and Dispositio n	36	1745-1752	2008
Tatsuki Fukami, Miki Nakajima, Taiga Maruichi, Shiori Takahashi, Howard L. McLeod, Masataka Takamiya, Yasuhiro Aoki, and Tsuyoshi Yokoi	Structure and characterization of human carboxylesterase 1A1, 1A2, and 1A3 genes.	Pharmacogenetics and Genomics	18	911-920	2008

Katsuhiko Mizuno, Miki Katoh, Hirotoshi Okumura, Nao Nakagawa, Toru Negishi, Takanori Hashizume, Miki Nakajima, and Tsuyoshi Yokoi	Mitabolic activation of benzodiazepine by CYP3A4.	Drug Metabolism and Disposition	37	345-351	2008
Shiori Takahashi, Miki Katoh, Takashi Saitoh, Miki Nakajima, and Tsuyoshi Yokoi	Species differences in carboxylesterase inhibition in rat and human.	Drug Metabolism and Disposition		In press	2008
Takuya Mohri, Miki Nakajima, Shingo Takagi and Tsuyoshi Yokoi;	MicroRNA regulates human vitamin D receptor.	International Journal of Cancer		In press	2008

VI. 研究成果の刊行物・別刷

Supplemental Material can be found at:
http://www.jbc.org/cgi/content/full/M709382200/DC1

THE JOURNAL OF BIOLOGICAL CHEMISTRY VOL. 283, NO. 15, pp. 9674–9680, April 11, 2008

Post-transcriptional Regulation of Human Pregnane X Receptor by Micro-RNA Affects the Expression of Cytochrome P450 3A4*[S]

Received for publication, November 15, 2007, and in revised form, February 7, 2008 Published, JBC Papers in Press, February 11, 2008, DOI 10.1074/jbc.M709382200

Shingo Takagi, Miki Nakajima, Takuya Mohri, and Tsuyoshi Yokoi[1]

From Drug Metabolism and Toxicology, Division of Pharmaceutical Sciences, Graduate School of Medical Science, Kanazawa University, Kakuma-machi, Kanazawa 920-1192, Japan

Pregnane X receptor (PXR) is a major transcription factor regulating the inducible expression of a variety of transporters and drug-metabolizing enzymes, including CYP3A4 (cytochrome P450 3A4). We first found that the PXR mRNA level was not correlated with the PXR protein level in a panel of 25 human livers, indicating the involvement of post-transcriptional regulation. Notably, a potential miR-148a recognition element was identified in the 3′-untranslated region of human PXR mRNA. We investigated whether PXR might be regulated by miR-148a. A reporter assay revealed that miR-148a could recognize the miR-148a recognition element of PXR mRNA. The PXR protein level was decreased by the overexpression of miR-148a, whereas it was increased by inhibition of miR-148a. The miR-148a-dependent decrease of PXR protein attenuated the induction CYP3A4 mRNA. Furthermore, the translational efficiency of PXR (PXR protein/PXR mRNA ratio) was inversely correlated with the expression levels of miR-148a in a panel of 25 human livers, supporting the miR-148a-dependent regulation of PXR in human livers. Eventually, the PXR protein level was significantly correlated with the CYP3A4 mRNA and protein levels. In conclusion, we found that miR-148a post-transcriptionally regulated human PXR, resulting in the modulation of the inducible and/or constitutive levels of CYP3A4 in human liver. This study will provide new insight into the unsolved mechanism of the large interindividual variability of CYP3A4 expression.

A key function of the liver is the metabolism and elimination of xenobiotics or endobiotics. The expression of genes involved in these processes is largely regulated by transcription factors belonging to the nuclear receptor family. Pregnane X receptor (PXR[2]; alternate names SXR, PAR, and NR1I2), a member of the nuclear receptor family, is a crucial regulator of drug metabolism and elimination. It is predominantly expressed in liver and small intestine. PXR is activated by a broad spectrum of xenobiotics, including antibiotics, antimycotics, and herbal components (1); dimerizes with retinoid X receptor α (RXRα); and binds to response elements of target genes, including cytochrome P450s, UDP-glucuronosyltransferases, glutathione *S*-transferases, sulfotransferases, and various transporters, such as MDR1 (multidrug resistance 1) and MRP-2 (multidrug resistance-associated protein 2) to induce them (2). Thus, PXR is recognized as a xenosensor for the detoxification of foreign compounds. However, it also plays a role as a physiological sensor of bile acids to protect the body from toxicity by regulating the expression of target genes that decreases the synthesis and increases the elimination of bile acids (3, 4).

One of the best known genes regulated by PXR is *CYP3A4*, the most abundant P450 in human liver that catalyzes the metabolism of over 50% of current prescription drugs (5–7). A large interindividual difference (~50-fold) has been reported for the CYP3A4 level in the general population (8), which cannot be explained by genetic polymorphisms (9, 10). The CYP3A4 expression is largely regulated at the transcriptional level by transcriptional factors, such as CCAAT/enhancer-binding proteins, C/EBPα and C/EBPβ, and hepatocyte nuclear factors, HNF4α and HNF3γ, as well as constitutive androstane receptor (CAR) and PXR (11). However, the cause of the large interindividual variability in CYP3A4 level is poorly understood and is an urgent issue to be solved. The regulation by PXR may, in part, be responsible for such variability, since PXR is activated by endogenous compounds, such as steroid hormones and bile acids (1, 12).

PXR regulates many targets controlling pharmacokinetics, but its own regulation is not fully understood, with reports showing only that human PXR is induced by dexamethasone through glucocorticoid receptor (13) or by clofibrate through peroxisome proliferator-activated receptor α (14). Employing an on-line search using the miRBase Target data base (15) (available on the World Wide Web), we found some potential recognition sites for micro-RNAs (miRNAs) in the 3′-untranslated region (UTR) of the human PXR.

miRNAs are a recently discovered family of short noncoding RNA whose final product is an ~22-nucleotide functional RNA

* This work was supported in part by a grant from the Ministry of Education, Science, Sports, and Culture of Japan, by Research on Toxicogenomics, Health and Labor Science Research Grants from the Ministry of Health, Labor, and Welfare of Japan, and by The Research Foundation for Pharmaceutical Sciences in Japan. The costs of publication of this article were defrayed in part by the payment of page charges. This article must therefore be hereby marked "*advertisement*" in accordance with 18 U.S.C. Section 1734 solely to indicate this fact.

[S] The on-line version of this article (available at http://www.jbc.org) contains supplemental Table 1 and Fig. 1.

[1] To whom correspondence should be addressed. Tel./Fax: 81-76-234-4407; E-mail: tyokoi@kenroku.kanazawa-u.ac.jp.

[2] The abbreviations used are: PXR, pregnane X receptor; AsO, antisense oligonucleotide; CAR, constitutive androstane receptor; miRNA, micro-RNA; RXRα, retinoid X receptor α; UTR, untranslated region; RT, reverse transcription; GAPDH, glyceraldehyde-3-phosphate dehydrogenase; snRNA, small nuclear RNA.

molecule (16). They play important roles in the regulation of target genes by binding to complementary regions of transcripts to repress their translation or regulate degradation. At present, more than 400 miRNAs have been identified in humans, and miRNAs are predicted to control about 30% of the genes within the human genome (17, 18). The roles of miRNAs have received attention especially in the cancer field but hardly yet in the field of pharmacokinetics. In the present study, we investigated whether human PXR might be post-transcriptionally regulated by miRNA and its impact on CYP3A4 expression.

EXPERIMENTAL PROCEDURES

Chemicals and Reagents—Rifampicin was obtained from Wako Pure Chemicals (Osaka, Japan). The pGL3-promoter vector, pGL4.74-TK plasmid, Tfx-20 reagent, and dual luciferase reporter assay system were purchased from Promega (Madison, WI). Lipofectamine 2000 and Lipofectamine RNAiMAX were from Invitrogen. Pre-miR miRNA precursors for miR-148a and for the negative control were from Ambion (Austin, TX). Locked nucleic acid-modified antisense oligonucleotides (AsOs) for miR-148a (5′-ACAAAGTTCTGTAGTGCACTGA-3′; locked nucleic acid is indicated by the underline) and for the negative control (5′-AGACUAGCGGUAUCUUAAACC-3′) were commercially synthesized at Greiner Bio-One (Tokyo, Japan). All primers and oligonucleotides were commercially synthesized at Hokkaido System Sciences (Sapporo, Japan). Goat anti-human PXR polyclonal antibodies (N-16), rabbit anti-human RXRα polyclonal antibodies (D-20), and goat anti-human HNF4α polyclonal antibodies (S-20) were from Santa Cruz Biotechnology, Inc. (Santa Cruz, CA). Rabbit anti-CYP3A4 polyclonal antibodies were from BD Gentest (Worburn, MA), and rabbit anti-human CAR polyclonal antibodies were from CHEMICON (Temecula, CA). Rabbit anti-human GAPDH polyclonal antibodies were from IMGENEX (San Diego, CA). Alexa Fluor 680 donkey anti-goat IgG was from Invitrogen. IRDye 680 goat anti-rabbit IgG was from LI-COR Biosciences (Lincoln, NE). All other chemicals and solvents were of the highest grade commercially available.

Human Livers and Cell Culture Conditions—Human liver samples from 25 donors were obtained from the Human and Animal Bridging Research Organization (Chiba, Japan). The human hepatocellular carcinoma cell lines HepG2 and HuH7 were obtained from Riken Gene Bank (Tsukuba, Japan), and HLE was from the Japanese Collection of Research Bioresources (Tokyo, Japan). The human colon carcinoma cell lines LS180 and Caco-2, the human embryonic kidney cell line HEK293, and the human breast adenocarcinoma cell line MCF-7 were obtained from American Type Culture Collection (Manassas, VA). HepG2, HuH7, and HLE cells were cultured in Dulbecco's modified Eagle's medium (Nissui Pharmaceutical, Tokyo, Japan) supplemented with 10% fetal bovine serum (Invitrogen). LS180, Caco-2, and MCF-7 cells were cultured in Dulbecco's modified Eagle's medium supplemented with 0.1 mM nonessential amino acid (Invitrogen) and 10% fetal bovine serum. Differentiated Caco-2 (Caco-2/D) cells were obtained by culture for 3 weeks postconfluence. HEK293 cells were cultured in Dulbecco's modified Eagle's medium supplemented with 4.5 g/liter glucose, 10 mM HEPES, and 10% fetal bovine serum. These cells were maintained at 37 °C under an atmosphere of 5% CO_2, 95% air.

Real Time RT-PCR for PXR and CYP3A4—Total RNA was isolated from 25 human liver samples using ISOGEN (Nippon Gene, Tokyo, Japan) according to the manufacturer's protocol. The cDNAs were synthesized from total RNA using ReverTra Ace (Toyobo, Osaka, Japan). The forward and reverse primers for CYP3A4 were 5′-CCAAGCTATGCTCTTCACCG-3′ and 5′-TCAGGCTCCACTTACGGTGC-3′, respectively. The forward and reverse primers for human PXR were 5′-TGCGAGATCACCCGGAAGAC-3′ and 5′-ATGGGAGAAGGTAGTGTCAAAGG-3′, respectively. The real time PCR was performed using the Smart Cycler (Cepheid, Sunnyvale, CA) with Smart Cycler software (version 1.2b) as follows. After an initial denaturation at 95 °C for 30 s, the amplification was performed by denaturation at 95 °C for 6 s and annealing and extension at 68 °C for 20 s for 40 cycles. The mRNA levels were normalized with GAPDH mRNA determined by real time RT-PCR, as described previously (19).

SDS-PAGE and Western Blot Analyses of PXR and CYP3A4—Whole cell lysates were prepared from 25 human liver samples by homogenization with lysis buffer (50 mM Tris-HCl (pH 8.0), 150 mM NaCl, 1 mM EDTA, 1% Nonidet P-40) containing protease inhibitors (0.5 mM (*p*-amidinophenyl)methanesulfonyl fluoride, 2 μg/ml aprotinin, 2 μg/ml leupeptin). The protein concentrations were determined using Bradford protein assay reagent (Bio-Rad) with γ-globulin as a standard. The whole cell lysates (10–50 μg) were separated with 7.5% SDS-polyacrylamide gel electrophoresis and transferred to Immobilon-P transfer membrane (Millipore, Bedford, MA). The membranes were probed with goat anti-human PXR, rabbit anti-human CYP3A4, goat anti-human HNF4α, rabbit anti-human CAR, or rabbit anti-human GAPDH antibodies and the corresponding fluorescent dye-conjugated second antibody, and the band densities were quantified with an Odyssey infrared imaging system (LI-COR Biosciences). Nuclear extracts (10 μg) from the HepG2 and LS-180 cells were also used to determine the PXR protein level.

Real Time RT-PCR for Mature miR-148a—For the quantification of mature miR-148a, polyadenylation and reverse transcription were performed using the NCode miRNA first strand cDNA synthesis kit (Invitrogen) according to the manufacturer's protocol. The forward primer for miR-148a was 5′-TCAGTGCACTACAGAACTTTGT-3′, and the reverse primer was the supplemented universal qPCR primer. The PCR analyses were performed as follows. After an initial denaturation at 95 °C for 30 s, the amplification was performed by denaturation at 95 °C for 10 s and annealing and extension at 64 °C for 10 s for 40 cycles. The mature miR-148a level was normalized with U6 snRNA determined by real time RT-PCR, as described previously (20).

Construction of Reporter Plasmids—To construct luciferase reporter plasmids, various target fragments were inserted into the XbaI site downstream of the luciferase gene in the pGL3-promoter vector. The sequence from 3362 to 3383 in the human PXR mRNA (5′-ACAGACTCTTACGTGGAGAGTGCACTGA-3′) was termed the miR-148a recognition element (PXRMRE148). The fragment containing three copies of the PXRMRE148 (5′-CTAGAAGCCACAGACTCTTACGTGGAG-

AGTGCACTGACCTGTAGAAGCCACAGACTCTTACGTG-GAGAGTGCACTGACCTGTAGAAGCCACAGACTCTTAC-GTGGAGAGTGCACTGACCTGTAT-3′; PXRMRE148 is underlined) was cloned into the pGL3-promoter vector (pGL3p/3×PXRMRE). The complementary sequence of three copies of the PXRMRE148 was also cloned into the pGL3-promoter plasmid (pGL3p/3×PXRMRE-Rev). A fragment containing the perfect matching sequence with the mature miR-148a, 5′-CTAGACAAAGTTCTGTAGTGCACTGAT-3′ (the matching sequence of miR-148a is underlined) was cloned into the pGL3-promoter vector (pGL3p/c-148a). The nucleotide sequences of the constructed plasmids were confirmed by DNA sequencing analyses.

Luciferase Assay—Various luciferase reporter plasmids (pGL3p) were transiently transfected with pGL4.74-TK plasmid into HEK293 or HepG2 cells. Briefly, the day before transfection, the cells were seeded into 24-well plates. After 24 h, 70 ng of pGL3p plasmid, 30 ng of pGL4.74-TK plasmid, and 4 pmol of the precursors for miR-148a or control were transfected into HEK293 cells using Lipofectamine 2000. For HepG2 cells, 80 ng of pGL3p plasmid, 20 ng of pGL4.74-TK plasmid, and 10 pmol of the AsOs for miR-148a or control were transfected using Tfx-20 reagent. After incubation for 48 h, the cells were resuspended in passive lysis buffer, and then the luciferase activity was measured with a luminometer (Wallac, Turku, Finland), using the dual luciferase reporter assay system.

Transfection of Precursor or Antisense for miR-148a into HepG2 and LS-180 Cells and Isolation of Nuclear Extract and Total RNA—To investigate the effect of miR-148a on the expression of PXR protein, 50 nM precursor or 50 nM AsO for miR-148a or control was transfected into HepG2 cells using Lipofectamine RNAiMAX. After 72 h, total RNA was isolated using ISOGEN, and the mature miR-148a levels were determined by Northern blotting as described above. Nuclear extract was isolated using the NE-PER nuclear and cytoplasmic extraction reagents (Pierce) according to the manufacturer's protocol. LS180 cells were transfected with 50 nM precursor for miR-148a or control using Lipofectamine RNAiMAX. After 72 h, the cells were treated with 50 μM rifampicin or 0.1% (v/v) Me_2SO for 24 h. Then total RNA and nuclear extract were isolated.

Evaluation of the Expression Level of PXR in HepG2 Using Reporter Construct Containing PXR-responsive Element—The reporter construct pCYP3A4-362-7.7K contains the promoter region (−362 to +11), including the ER6 (everted repeat separated by six nucleotides) motif and the distal enhancer region (−7836 to −7200), including the DR3 (direct repeat separated by three nucleotides) motif of the *CYP3A4* gene, to which PXR binds (21). The day before transfection, HepG2 cells were seeded into 24-well plates. After 24 h, 180 ng of pCYP3A4-362-7.7K, 20 ng of pGL4.74-TK plasmid, and various doses of the precursors and AsOs for miR-148a or control were transfected using Tfx-20 reagent. After incubation for 48 h, the cells were treated with 10 μM rifampicin or 0.1% Me_2SO for 24 h, and then the luciferase activity was measured.

Statistical Analyses—Statistical significance was determined by analysis of variance followed by Dunnett's multiple comparisons test or Tukey's method test. Comparison of two groups was made with an unpaired, two-tailed Student's *t* test. Correlation analyses were performed by Spearman's rank method. A value of $p < 0.05$ was considered statistically significant.

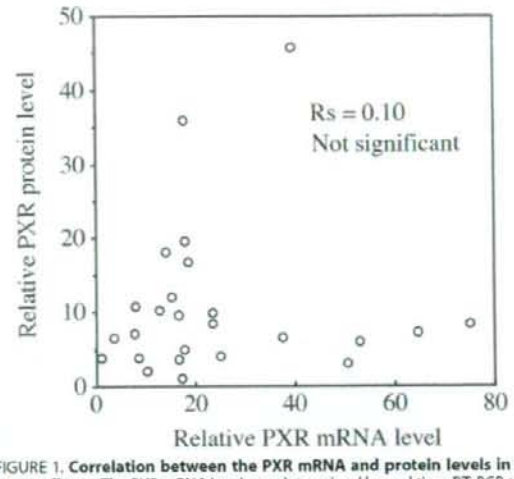

FIGURE 1. **Correlation between the PXR mRNA and protein levels in 25 human livers.** The PXR mRNA level was determined by real time RT-PCR and normalized with the GAPDH mRNA level. The PXR protein level was determined by Western blot analysis and normalized with the GAPDH protein level.

RESULTS

PXR Protein Level Is Not Associated with PXR mRNA Level in Human Livers—We first examined the PXR mRNA level in a panel of 25 human livers by real time RT-PCR assay and investigated the relationship with the PXR protein level. As shown in Fig. 1, no statistically significant correlation was observed between the PXR mRNA and protein levels ($Rs = 0.10$), indicating the involvement of post-transcriptional regulation of human PXR. To uncover the molecular mechanism of the post-transcriptional regulation, we sought to examine the involvement of miRNA-mediated regulation. Employing an on-line search using the miRBase Target data base (15) (available on the World Wide Web), potential recognition elements for 16 kinds of miRNA, such as miR-148a, miR-192, and miR-560, were found in the 3′-UTR in human PXR. Among them, we focused on miR-148a because it is selectively and abundantly expressed in liver (22) and has high complementarity in the 5′-end at miRNA-mRNA duplexes, including the seed sequence. The potential miR-148a target site is ~200 bases downstream of the stop codon of the human PXR mRNA. The alignment of hsa-miR-148a with the 3′-UTR of human PXR mRNA (Fig. 2*A*) was drawn using RNAhybrid (23) (available on the World Wide Web). We investigated whether this region, termed the miR-148a recognition element (PXRMRE148), might be involved in the regulation of PXR by miR-148a.

Expression Levels of miR-148a in Human Cancer Cell Lines—Real time RT-PCR analysis using the NCode miRNA first strand cDNA synthesis kit was performed to determine the expression levels of mature miR-148a in eight kinds of human cancer cell lines (Fig. 2*B*). The mature miR-148a was detected in all cell lines tested in this study, with large variability among cell lines (37-fold). The U6 snRNA levels, which were used for nor-

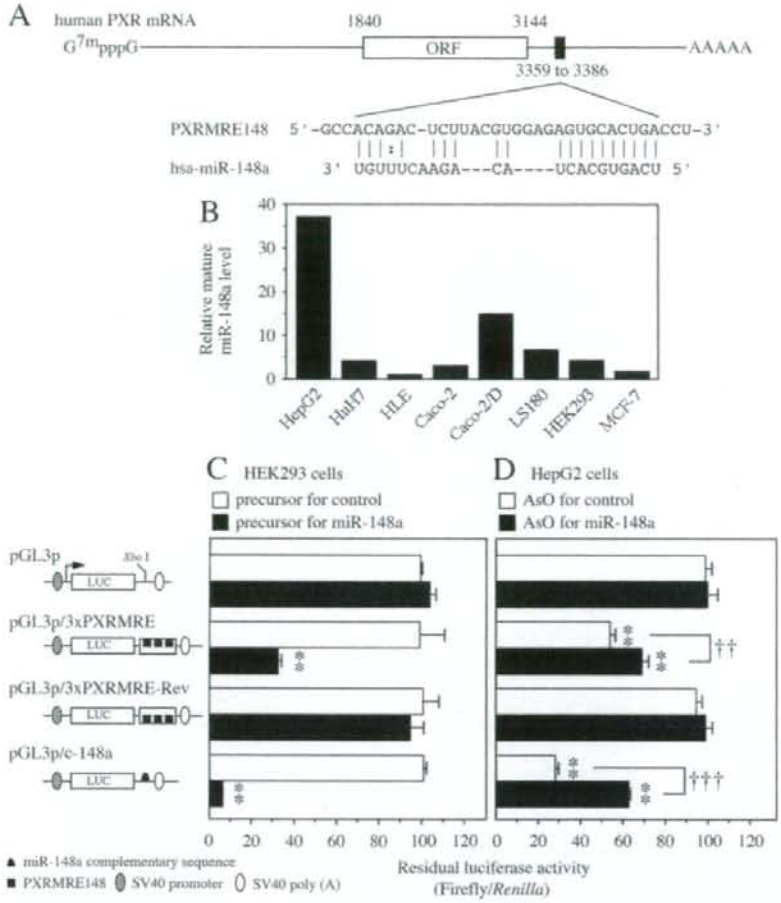

FIGURE 2. **Repressive regulation of human PXR by miR-148a.** *A*, complementarity of miR-148a to the predicted target sequence of human PXR. The potential miR-148a recognition element (PXRMRE148) is located on +3359 to +3386 in the 3'-UTR of human PXR mRNA, where the numbering refers to the 5'-end of mRNA as 1. *B*, the mature miR-148a levels in HepG2, HuH7, HLE, Caco-2, Caco-2/D (differentiated), LS180, HEK293, and MCF-7 cells were determined by real time RT-PCR analysis using an NCode miRNA first strand cDNA synthesis kit. The values were the mature miR-148a levels normalized with the U6 snRNA levels relative to that in HLE cells. *C* and *D*, luciferase assays were performed to investigate whether PXRMRE148 is functional in the regulation by miR-148a. The reporter constructs were transiently transfected with 4 pmol of the precursors for miR-148a or control into HEK293 cells (*C*) or 10 pmol of the AsO for miR-148a or control into HepG2 cells (*D*). The data were the firefly luciferase activities normalized with the *Renilla* luciferase activities relative to that of pGL3p plasmid. Each *column* represents the mean ± S.D. of three independent experiments. **, $p < 0.01$, compared with pGL3p; ††, $p < 0.01$; †††, $p < 0.001$, compared with AsO for control. *ORF*, open reading frame.

malization, varied <3-fold in the experiment, much less than the miR-148a levels. The mature miR-148a was higher in HepG2 and differentiated Caco-2 cells than the other cell lines. It was also interesting that, in Caco-2 cells, the expression level of mature miR-148a was increased with differentiation. Thus, the expression levels of mature miR-148a were highly variable among the human cancer cell lines.

Repressive Regulation of PXR by miR-148a in Human Cell Lines—To investigate whether PXRMRE148 is functional in the regulation by miR-148a, luciferase assays were performed with HEK293 cells (Fig. 2*C*). We first confirmed that the luciferase activity of the pGL3p/c-148a plasmid, in which the miR-148a complementary sequence was inserted downstream of the luciferase gene, was significantly ($p < 0.01$) decreased by the co-transfection with the precursor for miR-148a. The luciferase activity of pGL3p/3× PXRMRE plasmid, in which three copies of the potential miR-148a recognition site were inserted downstream of the luciferase gene, was also significantly ($p < 0.01$) decreased by co-transfection with the precursor for miR-148a (33% of control), whereas that of pGL3p/3× PXRMRE-Rev plasmid with the inverted recognition site was not affected. In HepG2 cells, which showed the highest expression of miR-148a (Fig. 2*B*), the luciferase activities of pGL3p/c-148a and pGL3p/3× PXRMRE plasmid were significantly ($p < 0.01$) lower than those of the control pGL3p plasmid (Fig. 2*D*). These activities were significantly ($p < 0.01$) restored by the transfection of AsO for miR-148a. These results underscore that miR-148a functionally recognizes PXRMRE148 to decrease the expression.

Effects of Overexpression or Inhibition of miR-148a on the PXR Protein Level in a Human Cell Line—We next examined the change in endogenous PXR protein expression by the overexpression or inhibition of miR-148a. By the transfection of the precursor for miR-148a into HepG2 cells that harbor the increased level of mature miR-148a, the PXR protein level was significantly ($p < 0.05$) decreased compared with the control (Fig. 3*A*). Conversely, by the transfection of the AsO for miR-148a into HepG2 cells, where the expression of mature miR-148a was extinguished, the PXR protein level was significantly ($p < 0.05$) increased compared with the control (Fig. 3*B*). Meanwhile, the expression level of RXRα protein, a heterodimer partner of PXR, was not affected by the overexpression or inhibition of miR-148a. It is well known that ligand-activated PXR activates the transcription of targets by binding to the responsive element. Using the pCYP3A4-362-7.7K plasmid containing the PXR-responsive element as a reporter construct, the changes in the PXR protein levels were monitored with the reporter activity (Fig. 3, *C* and *D*). The luciferase activity of pCYP3A4-362-7.7K plasmid was prominently (5.3-fold) increased by the treatment with rifampicin in HepG2 cells (Fig.

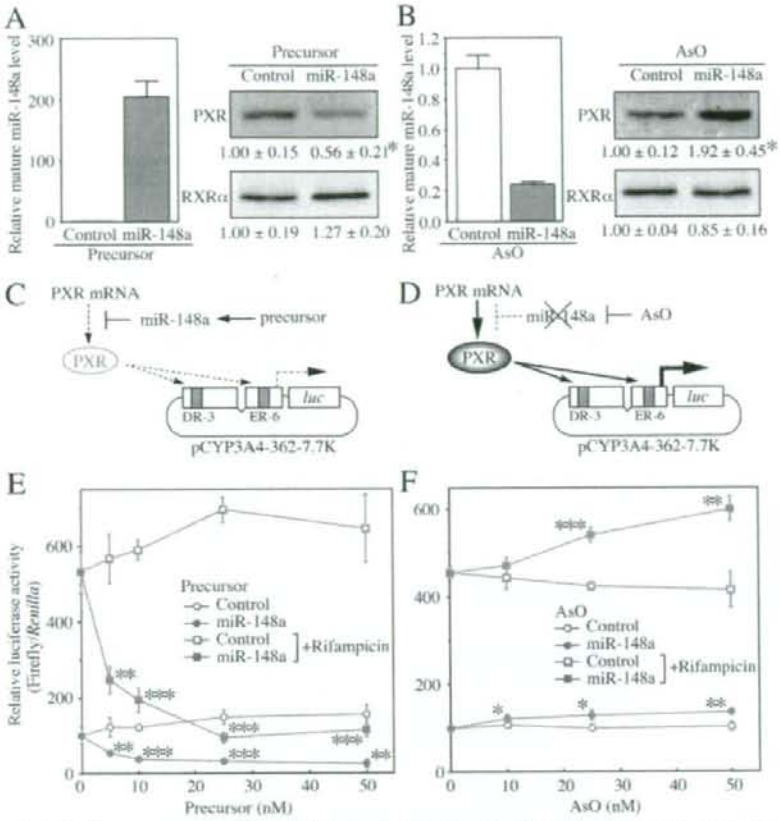

FIGURE 3. **Effects of overexpression or inhibition of miR-148a on the PXR protein level in HepG2 cells.** The precursors for miR-148a or control (50 nM) (*A*) or AsOs for miR-148a or control (50 nM) (*B*) were transfected into HepG2 cells. After 72 h, the cells were harvested, and total RNA and nuclear extracts were isolated. *A* and *B*, the mature miR-148a levels were determined by real time RT-PCR analyses. The values were the mature miR-148a levels normalized with the U6 snRNA levels relative to control. The PXR and RXRα protein levels in nuclear extracts were determined by Western blot analyses. The values are the mean ± S.D. for three independent experiments (*, $p < 0.05$, compared with control). *C* and *D*, schemes represent the principle of the reporter gene assay to evaluate the changes in the endogenous PXR protein level by the overexpression (*C*) or inhibition (*D*) of miR-148a. The pCYP3A4-362-7.7K plasmid contains the PXR-responsive elements, ER6 (−362 to +11) and DR3 (−7836 to −7200), of the *CYP3A4* gene upstream of the luciferase gene. *E* and *F*, the cells were transfected with the reporter plasmid and the precursors or AsOs. After 48 h, the cells were treated with 10 μM rifampicin (*squares*) or 0.1% Me_2SO (*circles*) for 24 h. The data were the firefly luciferase activities normalized with the *Renilla* luciferase activities relative to that of pGL3p plasmid without the precursors or AsOs. Each *point* represents the mean ± S.D. of three independent experiments. *, $p < 0.05$; **, $p < 0.01$; ***, $p < 0.001$, compared with control.

3*E*). Transfection of the precursor for miR-148a significantly decreased both the rifampicin-induced and basal transcriptional activities, resulting in a dose-dependent decrease of the induction. In contrast, the transfection of antisense for miR-148a significantly increased both the rifampicin-induced and basal transcriptional activity, resulting in a dose-dependent increase of the induction (Fig. 3*F*). These results suggest that miR-148a negatively regulates the expression of PXR protein and, subsequently, the induction of its targets.

Role of miR-148a-dependent PXR Regulation in the Induction of Endogenous CYP3A4 mRNA in a Human Cell Line—We next sought to examine whether the miR-148a-dependent change of the PXR protein level affects the CYP3A4 induction in human cells. LS-180 cells were used, because this cell line expressed relatively higher CYP3A4 mRNA than the other cell lines (data not shown). By the transfection of the precursor for miR-148a into the LS-180 cells, the PXR protein level was significantly ($p < 0.01$) decreased (Fig. 4*A*), concomitant with a dramatic increase of the mature miR-148a level, whereas the PXR mRNA level was not decreased at any time after the transfection (Fig. 4*B*). The RXRα protein level was not affected by the overexpression of miR-148a (Fig. 4*A*). As shown in Fig. 4*C*, the CYP3A4 mRNA level was significantly increased by the treatment with rifampicin (5.0-fold). However, this induction was diminished by the overexpression of miR-148a, although the basal CYP3A4 mRNA level was not affected. These results suggest that the miR-148a-dependent regulation of PXR affects the induction of CYP3A4.

The miR-148a-dependent PXR Regulation May Control CYP3A4 Expression in Human Liver Tissue—To further investigate the effects of the miR-148a-dependent regulation of PXR in human liver tissue, the relationships between the expression levels of miR-148a, PXR, and CYP3A4 were investigated using a panel of 25 human livers (supplemental Table 1). The expression levels of miR-148a were variable (95-fold) in the panel of human livers. The miR-148a level in liver sample 18 was comparable with that in HepG2 cells. The PXR mRNA (75-fold) and CYP3A4 mRNA (363-fold) were also variable. As shown in Fig. 1, the PXR mRNA level was not correlated with the PXR protein level. In contrast, the CYP3A4 mRNA level was significantly correlated ($Rs = 0.67, p < 0.001$) with the CYP3A4 protein level (Fig. 5*A*). When the PXR protein/PXR mRNA ratios were calculated as an index of the translational efficiency of PXR, they were inversely correlated with the miR-148a level ($Rs = -0.41, p < 0.05$) (Fig. 5*B*), suggesting that PXR is negatively regulated by miR-148a in human liver. The PXR protein level was significantly correlated with both the CYP3A4 mRNA level ($Rs = 0.47, p < 0.05$) (Fig. 5*C*) and the CYP3A4 protein level ($Rs = 0.67, p < 0.001$) (Fig. 5*D*). As summarized in Fig. 5*E*, the post-transcriptional regulation of PXR by miR-148a appeared to have substantial impact on the CYP3A4 level in human livers.

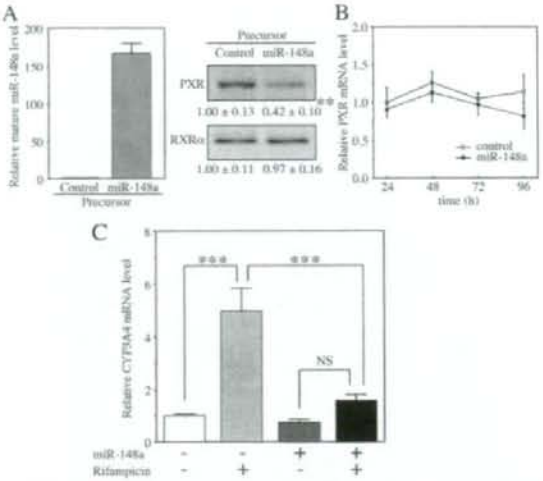

FIGURE 4. **Effects of overexpression of miR-148a on the induction of endogenous CYP3A4 mRNA in LS180 cells.** *A* and *B*, the precursors for miR-148a or control (50 nM) were transfected into LS180 cells. *A*, after 72 h, the cells were harvested, and total RNA and nuclear extracts were isolated. The mature miR-148a level was determined by real time RT-PCR analysis. The values are the mature miR-148a levels normalized with the U6 snRNA levels relative to control. The PXR and RXRα protein levels were determined by Western blot analysis. The values are the mean ± S.D. of three independent experiments (**, $p < 0.01$, compared with control). *B*, after 24, 48, 72, and 96 h, the cells were harvested, and total RNA was isolated. The PXR mRNA level was determined by real time RT-PCR analysis. The values are the PXR mRNA levels normalized with the GAPDH mRNA levels relative to control. Each point represents the mean ± S.D. of three independent experiments. *C*, precursor-transfected LS180 cells were treated with 50 μM rifampicin or 0.1% Me_2SO for 24 h, and then total RNA was isolated. The CYP3A4 mRNA levels were determined by real time RT-PCR and normalized with the GAPDH mRNA level. The data are relative to that with the precursor for the control without rifampicin. Each *column* represents the mean ± S.D. of three independent experiments. ***, $p < 0.001$; *NS*, not significant.

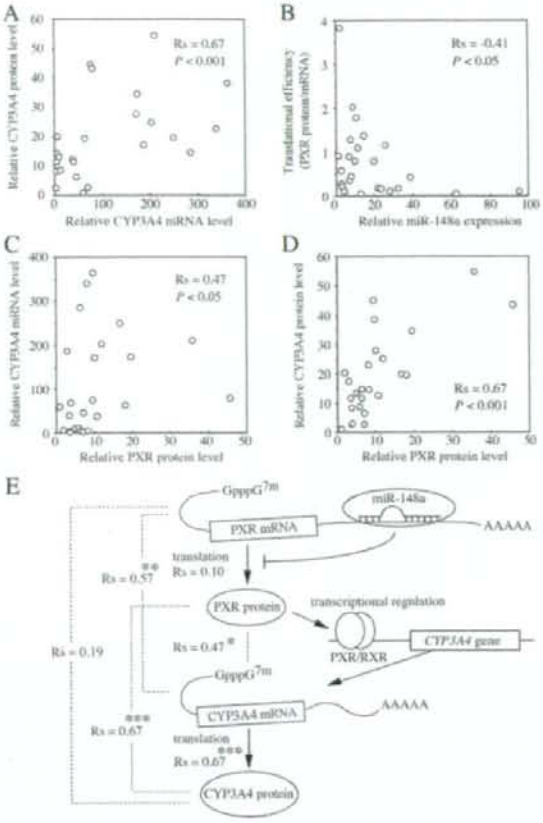

FIGURE 5. **Relationship between the expression levels of miR-148a, PXR, and CYP3A4 in human liver tissue.** *A*, the CYP3A4 mRNA level was significantly correlated with the CYP3A4 protein levels. *B*, the miR-148a level was inversely correlated with the translational efficiency of PXR (PXR protein/mRNA ratio). *C* and *D*, the PXR protein level was significantly correlated with the CYP3A4 mRNA (*C*) and protein level (*D*). *E*, summary of the correlation analyses (*, $p < 0.05$; **, $p < 0.01$; ***, $p < 0.001$).

DISCUSSION

PXR regulates at least 40 genes encoding proteins responsible for the metabolism and elimination of drugs (14). The study of PXR regulation assists in the understanding of the inter- and intraindividual variability in the pharmacokinetics of drugs. Although many research groups have found variability in the PXR mRNA levels in human liver samples, the correlation with its protein level has not fully been investigated. In this study, we first demonstrated that there was no significant correlation between them in human livers. For human PXR, two splicing variants, including exon 1b (PXR.2) or deleting the 5′-end of the exon 5 (PXR.3), have been reported (24, 25), which cannot be distinguished with our PCR primers. However, since the expression levels of these splicing variants were extremely low in our analysis (data not shown), consistent with a report by Lamba *et al.* (26), the dissociation of the PXR protein level with its mRNA level is not an artificial phenomenon. Identification of the miRNA recognition element in the human *PXR* gene suggested the involvement of miRNA in the regulation of PXR.

The luciferase assays showed that the endogenous and exogenous miR-148a negatively regulated the activity through PXRMRE148. In addition, the endogenous PXR protein level was diminished by the overexpression of miR-148a and elevated by its inhibition. These results clearly indicated that human PXR is post-transcriptionally regulated by miR-148a. The miR-148a-dependent changes of PXR protein affected the induction of CYP3A4 in LS180 cells. To further investigate whether the miR-148a affects the induction of other targets of PXR, we determined the expression levels of MDR1 and CYP2B6 in LS180 cells (data not shown). Rifampicin induced the MDR1 (5-fold) and CYP2B6 (2-fold) mRNAs, known targets of PXR (27, 28), and the induction was attenuated by the overexpression of miR-148a. Thus, the miR-148a-dependent regulation of PXR appeared to affect its target genes in common.

Interestingly, the miR-148a recognition element is also present in the 3′-UTR of CYP3A4 mRNA. The complementarity of CYP3A4 with miR-148 (score 15.48, energy −24.27) was higher than that of human PXR (score 15.14, energy −19.52). To investigate whether CYP3A4 is directly regulated by miR-148a, luciferase assays were performed using a plasmid containing three copies of the miR-148a recognition element in the

CYP3A4 gene. However, unlike the PXRMRE, the element in CYP3A4 did not respond to miR-148a (supplemental Fig. 1), indicating that CYP3A4 is not directly regulated by miR-148a.

In the panel of human livers, the expression level of miR-148a was inversely correlated with the translational efficiency of PXR, supporting the role of miR-148a in the regulation of PXR in liver. The significant correlation between the CYP3A4 mRNA and the CYP3A4 protein level in human livers in this study, in accordance with previous studies (29, 30), supported the finding that miRNA did not directly regulate the CYP3A4 expression. The PXR protein level was correlated with the CYP3A4 mRNA level in human liver, indicating that miR-148a affects the CYP3A4 expression through modulating PXR expression. The PXR protein level was not correlated with the CYP2B6 ($Rs = 0.31$, $p > 0.1$) or MDR1 ($Rs = -0.20$, $p > 0.3$) mRNA levels in the panel of human livers (data not shown), in contrast to CYP3A4. Thus, we speculate that the PXR does not largely affect the constitutive expression of CYP2B6 and MDR1 in the liver. In our panel of human livers, the CYP3A4 mRNA level was not correlated with the HNF4α protein level ($Rs = -0.14$, $p > 0.5$) or CAR protein level ($Rs = 0.12$, $p > 0.5$), indicating a significant contribution of PXR to the constitutive CYP3A4 level.

Most of the genes in the vertebrate nuclear receptor superfamily are strongly conserved between species. The ligand-binding domain of PXR shares amino acid identity of 75% between human and rodent, which can explain why the key ligands for PXR vary across species. Meanwhile, the DNA-binding domain of PXR shares more than 95% amino acid identity (1), inducing a similar set of genes. Most miRNAs are evolutionally conserved, which suggests that the miRNA-mediated regulation of certain genes would be common among species. The MRE148 is also identified in the 3′-UTR in mouse PXR (score 16.63, energy −21.4) and rat PXR (score and energy are not calculated at miRBase, but it has only a 1-base difference from the corresponding mouse sequence) at −670 bp downstream of the stop codon, although the 3′-UTR of PXR is poorly conserved between humans and rodents. It is therefore possible that rodent PXR may also be regulated by miR-148a, suggesting that rodents might be useful model animals to investigate the role of miR-148a in drug metabolism and elimination *in vivo*.

In conclusion, we found that human PXR is post-transcriptionally regulated by miR-148a affecting the CYP3A4 level in human liver. This study would provide new insight into the unsolved mechanism of the large interindividual variability of CYP3A4 expression.

Acknowledgments—We are grateful to Drs. Kiyoshi Nagata and Yasushi Yamazoe (Division of Drug Metabolism and Molecular Toxicology, Graduate School of Pharmaceutical Sciences, Tohoku University, Sendai, Japan) for providing pCYP3A4-362-7.7K plasmid. We acknowledge Brent Bell for reviewing the manuscript.

REFERENCES

1. Kliewer, S. A., Goodwin, B., and Willson, T. M. (2002) *Endocr. Rev.* **23,** 687–702
2. Meijerman, I., Beijnen, J. H., and Schellens, J. H. (2006) *Oncologist* **11,** 742–752
3. Staudinger, J. L., Goodwin, B., Jones, S. A., Hawkins-Brown, D., MacKenzie, K. I., LaTour, A., Liu, Y., Klaassen, C. D., Brown, K. K., Reinhard, J., Willson, T. M., Koller, B. H., and Kliewer, S. A. (2001) *Proc. Natl. Acad. Sci. U. S. A.* **98,** 3369–3374
4. Xie, W., Radominska-Pandya, A., Shi, Y., Simon, C. M., Nelson, M. C., Ong, E. S., Waxman, D. J., and Evans, R. M. (2001) *Proc. Natl. Acad. Sci. U. S. A.* **98,** 3375–3380
5. Blumberg, B., Sabbagh, W., Jr., Juguilon, H., Bolado, J., Jr., van Meter, C. M., Ong, E. S., and Evans, R. M. (1998) *Genes Dev.* **12,** 3195–3205
6. Lehmann, J. M., McKee, D. D., Watson, M. A., Willson, T. M., Moore, J. T., and Kliewer, S. A. (1998) *J. Clin. Invest.* **102,** 1016–1023
7. Goodwin, B., Hodgson, E., and Liddle, C. (1999) *Mol. Pharmacol.* **56,** 1329–1339
8. Ozdemir, V., Kalowa, W., Tang, B. K., Paterson, A. D., Walker, S. E., Endrenyi, L., and Kashuba, A. D. (2000) *Pharmacogenetics* **10,** 373–388
9. Lamba, J. K., Lin, Y. S., Thummel, K., Daly, A., Watkins, P. B., Strom, S., Zhang, J., and Schuetz, E. G. (2002) *Pharmacogenetics* **12,** 121–132
10. Floyd, M. D., Gervasini, G., Masica, A. L., Mayo, G., George, A. L., Jr., Bhat, K., Kim, R. B., and Wilkinson, G. R. (2003) *Pharmacogenetics* **13,** 595–606
11. Martínez-Jiménez, C. P., Jover, R., Donato, M. T., Castell, J. V., and Gómez-Lechón, M. J. (2007) *Curr. Drug Metab.* **8,** 185–194
12. Kretschmer, X. C., and Baldwin, W. S. (2005) *Chem. Biol. Interact.* **155,** 111–128
13. Pascussi, J. M., Drocourt, L., Fabre, J. M., Maurel, P., and Vilarem, M. J. (2000) *Mol. Pharmacol.* **58,** 361–372
14. Aouabdi, S., Gibson, G., and Plant, N. (2006) *Drug Metab. Dispos.* **34,** 138–144
15. Griffiths-Jones, S. (2004) *Nucleic Acids Res.* **32,** D109–D111
16. Bartel, D. P. (2004) *Cell* **116,** 281–297
17. Lewis, B. P., Burge, C. B., and Bartel, D. P. (2005) *Cell* **120,** 15–20
18. Xie, X., Lu, J., Kulbokas, E. J., Golub, T. R., Mootha, V., Lindblad-Toh, K., Lander, E. S., and Kellis, M. (2005) *Nature* **434,** 338–345
19. Tsuchiya, Y., Nakajima, M., Kyo, S., Kanaya, T., Inoue, M., and Yokoi, T. (2004) *Cancer Res.* **64,** 3119–3125
20. Tsuchiya, Y., Nakajima, M., Takagi, S., Taniya, T., and Yokoi, T. (2006) *Cancer Res.* **66,** 9090–9098
21. Takada, T., Ogino, M., Miyata, M., Shimada, M., Nagata, K., and Yamazoe, Y. (2004) *Drug Metab. Pharmacokinet.* **19,** 103–113
22. Barad, O., Meiri, E., Avniel, A., Aharonov, R., Barzilai, A., Bentwich, I., Einav, U., Gilad, S., Hurban, P., Karov, Y., Lobenhofer, E. K., Sharon, E., Shiboleth, Y. M., Shtutman, M., Bentwich, Z., and Einat, P. (2004) *Genome Res.* **14,** 2486–2494
23. Rehmsmeier, M., Steffen, P., Hochsmann, M., and Giegerich, R. (2004) *RNA* **10,** 1507–1517
24. Bertilsson, G., Heidrich, J., Svensson, K., Asman, M., Jendeberg, L., Sydow-Bäckman, M., Ohlsson, R., Postlind, H., Blomquist, P., and Berkenstam, A. (1998) *Proc. Natl. Acad. Sci. U. S. A.* **95,** 12208–12213
25. Dotzlaw, H., Leygue, E., Watson, P., and Murphy, L. C. (1999) *Clin. Cancer Res.* **5,** 2103–2107
26. Lamba, V., Yasuda, K., Lamba, J. K., Assem, M., Davila, J., Strom, S., and Schuetz, E. G. (2004) *Toxicol. Appl. Pharmacol.* **199,** 251–265
27. Synold, T. W., Dussault, I., and Forman, B. M. (2001) *Nat. Med.* **7,** 584–590
28. Goodwin, B., Moore, L. B., Stoltz, C. M., McKee, D. D., and Kliewer, S. A. (2001) *Mol. Pharmacol.* **60,** 427–431
29. Westlind-Johnsson, A., Malmebo, S., Johansson, A., Otter, C., Andersson, T. B., Johansson, I., Edwards, R. J., Boobis, A. R., and Ingelman-Sundberg, M. (2003) *Drug Metab. Dispos.* **31,** 755–761
30. Watanabe, M., Kumai, T., Matsumoto, N., Tanaka, M., Suzuki, S., Satoh, T., and Kobayashi, S. (2004) *J. Pharmacol. Sci.* **94,** 459–462

Allosteric Kinetics of Human Carboxylesterase 1: Species Differences and Interindividual Variability

SHIORI TAKAHASHI, MIKI KATOH, TAKASHI SAITOH, MIKI NAKAJIMA, TSUYOSHI YOKOI

Drug Metabolism and Toxicology, Division of Pharmaceutical Sciences, Graduate School of Medical Science, Kanazawa University, Kanazawa 920-1192, Japan

Received 29 November 2007; revised 29 January 2008; accepted 4 February 2008

Published online 27 March 2008 in Wiley InterScience (www.interscience.wiley.com). DOI 10.1002/jps.21376

ABSTRACT: Esterified drugs such as imidapril, derapril, and oxybutynin hydrolyzed by carboxylesterase 1 (CES1) are extensively used in clinical practice. The kinetics using the CES1 substrates have not fully clarified, especially concerning species and tissue differences. In the present study, we performed the kinetic analyses in humans and rats in order to clarify these differences. The imidaprilat formation from imidapril exhibited sigmoidal kinetics in human liver microsomes (HLM) and cytosol (HLC) but Michaelis-Menten kinetics in rat liver microsomes and cytosol. The 2-cyclohexyl-2-phenylglycolic acid (CPGA) formation from oxybutynin were not detected in enzyme sources from rats, although HLM showed high activity. The kinetics were clarified to be different among species, tissues, and preparations. In individual HLM and HLC, there was large interindividual variability in imidaprilat (31- and 24-fold) and CPGA formations (15- and 9-fold). Imidaprilat formations exhibited Michaelis-Menten kinetics in HLM and HLC with high activity but sigmoidal kinetics in those with low activity. CPGA formations showed sigmoidal kinetics in high activity HLM but Michaelis-Menten kinetics in HLM with low activity. We revealed that the kinetics were different between individuals. These results could be useful for understanding interindividual variability and for the development of oral prodrugs. © 2008 Wiley-Liss, Inc. and the American Pharmacists Association J Pharm Sci 97:5434–5445, 2008

Keywords: phase I enzyme; prodrugs; enzyme kinetics; phase I metabolism

INTRODUCTION

Carboxylesterase (CES) is one of the phase I drug metabolizing enzymes and is responsible for the hydrolysis of many ester- and amido-type compounds. CES belongs to a serine hydrolase superfamily and is expressed in various mammalian tissues.[1] Mammalian CESs are mainly expressed in liver and small intestine.[2] Recently, human CES was clarified to be expressed in cytosol as well as microsomes in our laboratory.[3] In humans, there are two major isoforms, CES1 and CES2. The human CES1 gene spans approximately 30 kb on chromosome 16q13-q22.1 and has 14 exons.[4] CES1 is mainly expressed in the liver but also in the small intestine at low expression levels.[5] CES1 plays an important role in the metabolism and bioactivation of esterified prodrugs such as capecitabine,[3] imidapril,[6] methylphenidate,[7] and oseltamivir.[8] Esterification is one of the beneficial approaches to increase the oral bioavailability or reduce the adverse reactions of drugs. Therefore, CES1 can be a major

Shiori Takahashi and Miki Katoh contributed equally to this work.

Abbreviations: CES, carboxylesterase; CPGA, 2-cyclohexyl-2-phenylglycolic acid; HLM, human liver microsomes; HLC, human liver cytosol; HJM, human jejunum microsomes; HJC, human jejunum cytosol; RLM, rat liver microsomes; RLC, rat liver cytosol; RJM, rat jejunum microsomes; RJC, rat jejunum cytosol; LC-MS/MS, liquid chromatography-tandem mass spectrometry; BNPP, bis (*p*-nitrophenyl) phosphate; CYP, cytochrome P450; SNP, single nucleotide polymorphism.

Correspondence to: Tsuyoshi Yokoi (Telephone: +81-76-234-4407; Fax: +81-76-234-4407;
E-mail: tyokoi@kenroku.kanazawa-u.ac.jp)

Journal of Pharmaceutical Sciences, Vol. 97, 5434–5445 (2008)

determinant of the pharmacological and toxicological effects of prodrugs. Understanding the CES function is necessary to predict the pharmacokinetics of prodrugs. Kinetic analyses are helpful to characterize the enzymatic properties of CES1. The typical CES1 substrates are imidapril, derapril, and oxybutynin, which are clinically used in Japan. Imidapril and derapril are angiotensin-converting enzyme inhibitors and oxybutynin is an anticholinergic drug. Imidapril, derapril, and oxybutynin are hydrolyzed to imidaprilat,[9] deraprilat,[10] and 2-cyclohexyl-2-phenylglycolic acid (CPGA),[11] respectively. In the present study, we selected these three drugs as typical CES1 substrates.

Mammalian CES activities are present in various tissues such as liver, small intestine, lung and blood, and the liver shows the highest hydrolase activity.[12] Some compounds are hydrolyzed by mammalian CESs in microsomes from liver and intestine.[12] In comparison with human CES, there are many isoforms in rats and mice.[12] In addition, as reported by Li et al.,[13] CES was not present in human plasma although it was highly expressed in that of rodents indicating differences in the localization of CES expression between mammalians. Recently, species differences in the pyrethroid hydrolysis reaction have been reported.[14,15] However, sufficient kinetic analyses of the hydrolysis reaction by CES concerning species and tissue differences have not been performed. It is still unclear whether cytosolic CES exhibits similar kinetics to microsomal CES. For drug development, it is important to elucidate the species and tissue differences in CES kinetics. The purpose of the present study was to clarify the kinetics of CES1 hydrolase activity in human liver, human jejunum, rat liver, and rat jejunum. In addition, the differences in microsomal and cytosolic CES1 kinetics were investigated.

MATERIALS AND METHODS

Materials

Imidapril and imidaprilat (a major metabolite of imidapril) were kindly supplied by Tanabe Seiyaku (Osaka, Japan). Derapril was kindly provided by Takeda Pharmaceutical (Osaka, Japan). Oxybutynin, CPGA (a metabolite of oxybutynin), phenytoin, and clonazepam were obtained from Wako Pure Chemicals (Osaka, Japan). Pooled human liver microsomes (pooled HLM), pooled human liver cytosol (pooled HLC), microsomes from 13 individual human livers, and cytosol from 13 individual human livers were purchased from BD Gentest (Woburn, MA). Pooled human jejunum microsomes (pooled HJM) and cytosol (pooled HJC) were obtained from KAC (Shiga, Japan). All other chemicals and solvents were of analytical or the highest grade commercially available.

Preparation of Microsomes and Cytosol from Rat Liver or Jejunum

Wister rats, 7 weeks old, were obtained from Japan SLC, Inc. (Shizuoka, Japan). Pooled microsomes and cytosol from 5 rat livers (RLM and RLC) and jejunums (RJM and RJC) were prepared according to the method of Emoto et al.[16]

Imidaprilat Formation

Imidaprilat formation from imidapril was determined according to the method of Mabuchi et al.[17] with slight modifications. A typical incubation mixture (200 μL of total volume) contained the enzyme source and 100 mM tris(hydroxymethyl)aminomethane-HCl buffer (pH 7.4). After a 2-min preincubation at 37°C, the reaction was initiated by the addition of imidapril and then the mixture was incubated at 37°C for 30 min except for RLM and RLC (10 min). The reaction was terminated by adding 100 μL of ice-cold acetonitrile. After centrifugation at 9000*g* for 5 min, 10 μL of the supernatant were subjected to liquid chromatography-tandem mass spectrometry (LC-MS/MS) system.

LC was performed using an HP 1100 system including a binary pump, an automatic sampler, and a column oven (Agilent Technologies, Waldbronn, Germany), which was equipped with an Inertsil ODS-3 analytical column (2.1 × 100 mm; GL Science, Tokyo, Japan). The column temperature was 40°C and the flow rate was 0.2 mL/min. The mobile phase consisted of acetonitrile/10 mM ammonium formate, 20:80 (v/v). The LC was connected to a PE Sciex API 2000 tandem mass spectrometer (Applied Biosystems, Langen, Germany) operated in the positive electrospray ionization mode. The turbo gas was maintained at 500°C. Nitrogen was used as the nebulizing gas, turbo gas, and curtain gas at 40, 80, and 30 psi, respectively. Parent and/or fragment ions were filtered in the first quadrupole and dissociated in the collision cell using nitrogen as the collision

gas. The collision energy was 27 V. The mass/charge (m/z) ion transitions were recorded in the multiple reaction monitoring mode: m/z 378.2 and 206.3 for imidaprilat. The retention time of imidaprilat was 2.2 min. The limit of detection for imidaprilat was 0.2 pmol. The limit of quantification in the reaction mixture was 20 nM with CV's < 10%. In the preliminary study, a specific CES inhibitor, bis (p-nitrophenyl) phosphate (BNPP) (300 μM) inhibited the imidaprilat formation with all enzyme sources at 150 μM imidapril. A CES2 inhibitor, loperamide (20 and 200 μM) did not inhibit the imidaprilat formation in pooled HLM and HLC at 10 and 100 μM imidapril.

Deraprilat Formation

Deraprilat formation from derapril was determined according to the method of Ito et al.[18] with slight modifications. A typical incubation mixture (200 μL of total volume) contained the enzyme source and 100 mM tris(hydroxymethyl)aminomethane-HCl buffer (pH 7.4). Derapril was dissolved in methanol. The final concentration of methanol in the reaction mixture was <1.0%. After a 2-min preincubation at 37°C, the reaction was initiated by the addition of derapril and then the mixture was incubated for 30 min at 37°C. The reaction was terminated by adding 200 μL of ice-cold acetonitrile. Clonazepam (1 nmol) was added as an internal standard. After centrifugation at 9000g for 5 min, 50 μL of the supernatant was subjected to high-performance liquid chromatography equipped with a CAPCELL PAK CN UG120 analytical column (4.6 × 150 mm; Shiseido, Tokyo, Japan). The eluent was monitored at 210 nm with a noise-base clean Uni-3 (Union, Gunma, Japan). Deraprilat was quantified using a standard curve of derapril because authentic deraprilat could not be obtained. The column temperature was 35°C and the flow rate was 1.0 mL/min. The mobile phase consisted of acetonitrile/100 mM KH_2PO_4 (pH 3.0), 25:75 (v/v). The retention times of deraprilat and clonazepam were 6.1 and 11.4 min, respectively. In the preliminary study, BNPP (20 μM) inhibited the deraprilat formation with all enzyme sources at 10 μM derapril.

CPGA Formation

CPGA formation from oxybutynin was determined according to the method of Malcolm et al.[19] with slight modifications. A typical incubation mixture (200 μL of total volume) contained the enzyme source and 100 mM potassium phosphate buffer (pH 7.4). After a 2-min preincubation at 37°C, the reaction was initiated by the addition of oxybutynin and then the mixture was incubated for 30 min at 37°C. The reaction was terminated by adding 200 μL of ice-cold acetonitrile. Phenytoin (1 nmol) was added as an internal standard. After centrifugation at 9000g for 5 min, 90 μL of the supernatant was subjected to high-performance liquid chromatography equipped with a Develosil C30-UG-5 analytical column (4.6 × 150 mm; Nomura chemical, Aichi, Japan). The eluent was monitored at 220 nm. The column temperature was 35°C and the flow rate was 1.0 mL/min. The mobile phase consisted of acetonitrile/20 mM potassium phosphate buffer (pH 5.0), 40:60 (v/v). The retention times of CPGA and phenytoin were 6.2 and 11.1 min, respectively. The limit of detection for CPGA was 20 pmol. In the preliminary study, BNPP (5 μM) inhibited the CPGA formation with all enzyme sources at 200 μM oxybutynin. Loperamide (20 and 200 μM) did not inhibit the CPGA formation in pooled HLM and HLC at 10 and 100 μM oxybutynin.

Kinetic Analyses of Imidaprilat, Deraprilat, and CPGA Formation

The kinetic analyses were performed using pooled HLM, pooled HLC, RLM, RLC, RJM, and RJC. When the kinetic parameters were determined, the substrate concentrations ranged from 2 to 500 μM for imidapril, from 5 to 1000 μM for derapril, and from 4 to 500 μM for oxybutynin. The imidaprilat formation in HJM and that in HJC were examined at 200 μM imidapril. The protein concentrations of microsomes and cytosol were 0.2 and 1.0 mg/mL, respectively. The protein concentrations of RLM and RLC in the imidaprilat formations were 0.01 and 0.05 mg/mL, respectively. In the preliminary study, the linearity of the protein concentrations and incubation times were confirmed. The kinetic parameters were estimated from the fitted curves using a KaleidaGraph computer program (Synergy, Reading, PA) designed for nonlinear regression analysis. The following equations were used: Michaelis-Menten equation: $V = V_{max} \times [S]/(K_m + [S])$ and Hill equation: $V = (V_{max} \times [S]^n)/(S_{50}^n + [S]^n)$, where V is the velocity of the reaction, S is the substrate

concentration, K_m is the Michaelis-Menten constant, V_{max} is the maximum velocity, S_{50} is the substrate concentration showing the half-V_{max}, and n is Hill coefficient. Intrinsic clearance was calculated as V_{max}/K_m for the Michaelis-Menten kinetics. For the sigmoidal kinetics, the maximum clearance (CL_{max}) was calculated as $V_{max} \times (n-1)/S_{50} \times n(n-1)^{1/n}$ to estimate the highest clearance.[20]

Species and Tissue Differences in CPGA Formation

The CPGA formation was examined at 200 μM oxybutynin in pooled HLM, pooled HLC, pooled HJM, pooled HJC, RLM, RLC, RJM, and RJC. The protein concentrations of microsomes and cytosol were 0.5 and 2.5 mg/mL, respectively.

Interindividual Variability in Imidaprilat and CPGA Formation

Imidaprilat formation and that of CPGA were examined at 20 μM imidapril and 20 μM oxybutynin in 13 HLM and 13 HLC. The protein concentrations of HLM and HLC were 0.2 and 1.0 mg/mL, respectively. For the kinetic analysis of the imidaprilat formation, the individual HLM and HLC that could yield sufficient volumes were used as follows: HLM with high activities (HG3 and HH31), HLM with low activities (HH47 and HG64), HLC with high activities (HH18 and HG89), and HLC with low activities (HH47 and HH31). For the kinetic analysis of the CPGA formation, the individual HLM and HLC were used as follows: HLM and HLC with high activities (HG3 and HH18) and HLM and HLC with low activities (HH47 and HG64).

Statistical Analysis

The correlations between imidaprilat and CPGA formation in individual HLM or HLC were determined by Pearson's product moment method. A p value of less than 0.05 was considered statistically significant.

RESULTS

Kinetic Analysis of Imidaprilat Formation in Human Liver, Rat Liver, and Rat Jejunum

To investigate the differences in the CES1 characteristics between humans and rats or liver and jejunum, kinetic analyses of the imidaprilat formation were carried out in pooled HLM, pooled HLC, RLM, RLC, RJM, and RJC. Kinetic parameters were different between human and rat livers or rat livers and jejunums (Tab. 1). As shown in Figure 1, Eadie-Hofstee plots in pooled HLM and HLC exhibited curved lines at low substrate concentrations although the Hill coefficients were close to 1.0. The apparent S_{50} value in pooled HLM was lower than that of pooled HLC (Tab. 1). The kinetics in RLM and RLC fitted to the Michaelis-Menten equation and the V_{max}/K_m value of RLM was approximately two-fold higher

Table 1. Kinetic Parameters of Imidaprilat Formation in HLM, HLC, RLM, RLC, RJM, and RJC

	High Affinity Isoform			Low Affinity Isoform			
Enzyme Source	K_m (μM)	V_{max} (nmol/min/mg)	V_{max}/K_m (μL/min/mg)	K_m (μM)	V_{max} (nmol/min/mg)	V_{max}/K_m (μL/min/mg)	n
HLM	—	—	—	245[a]	2.4	7.4[b]	1.1 (1.1[c])
HLC	—	—	—	397[a]	0.2	0.5[b]	1.0 (1.1[c])
HJM	—	ND	—	—	—	—	—
HJC	—	ND	—	—	—	—	—
RLM	52	76.6	1459	—	—	—	—
RLC	33	22.4	677	—	—	—	—
RJM	41	1.0	25	346	3.7	10.6	—
RJC	53	0.2	4	382	0.8	2.1	—

n, Hill coefficient calculated using all concentrations of imidapril.
ND; not detected.
[a] S_{50}.
[b] CL_{max}.
[c] Hill coefficient calculated below 100 μM imidapril.

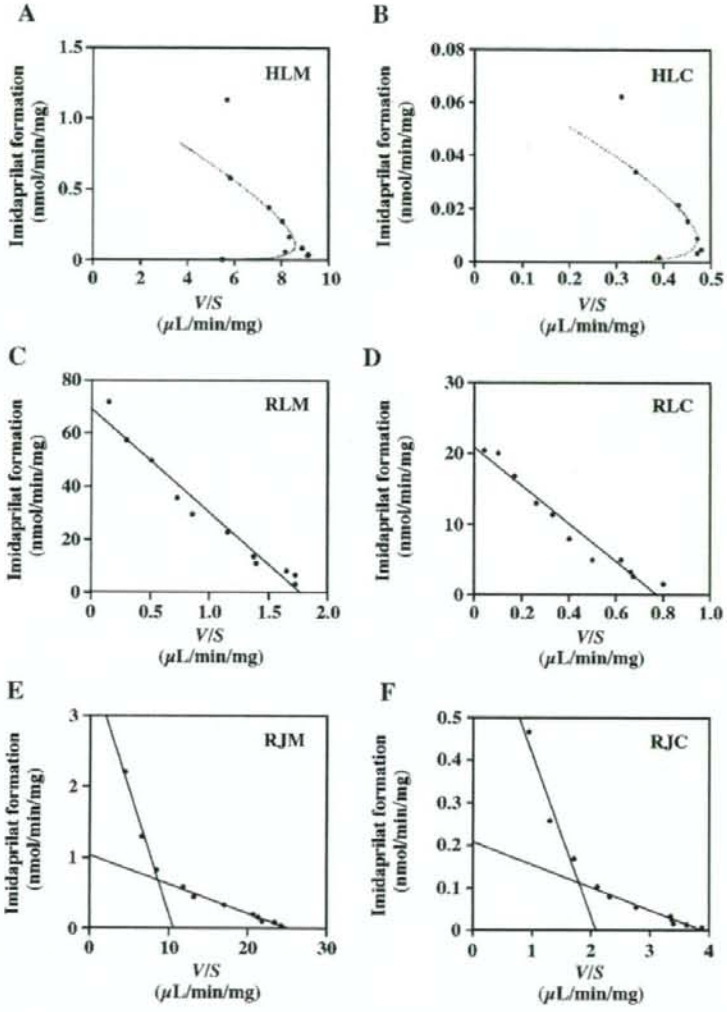

Figure 1. Kinetic analyses of imidaprilat formation catalyzed by pooled HLM (A), pooled HLC (B), RLM (C), RLC (D), RJM (E), and RJC (F). The concentration of imidapril was 2–500 μM. The curved lines (A and B) were estimated by the concentration below 100 μM imidapril. Each data point represents the mean of duplicate determinations.

than that of RLC. RLM and RLC hydrolyzed imidapril more efficiently than pooled HLM and HLC. RJM and RJC appeared bi-phasic in the Eadie-Hofstee plots. The apparent K_m values in RJM and RJC were similar in high and low affinity isoforms, but the V_{max} values of both isoforms in RJM were approximately five-fold higher than those in RJC. Imidaprilat formation in pooled HJM and HJC could not be detected.

Interindividual Variability of Imidaprilat Formation in HLM and HLC

Imidaprilat formation in microsomes from 13 human livers and in cytosol from 13 human livers was determined at 20 μM imidapril (Fig. 2). The interindividual variability of imidaprilat formation in HLM and HLC was 31- and 24-fold, respectively. The imidaprilat formation in HLM

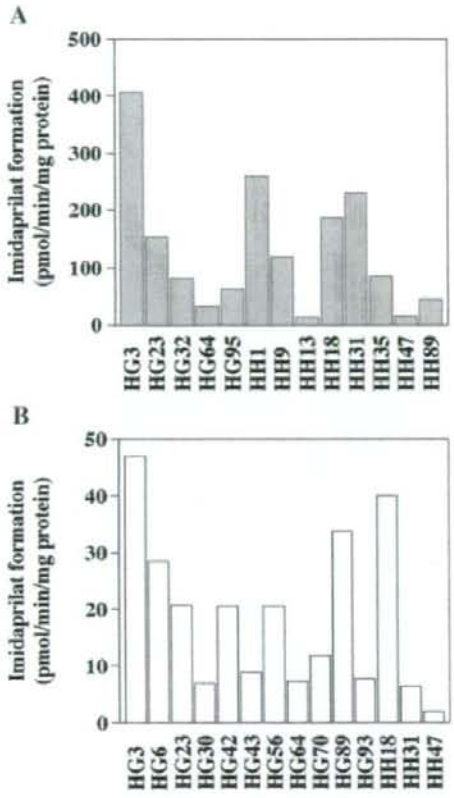

Figure 2. Interindividual variability of imidaprilat formation in 13 HLM (A) and in 13 HLC (B). The concentration of imidapril was 20 μM. Each column represents the mean of duplicate determinations.

ranged from 13.2 pmol/min/mg protein in HH13 to 406.9 pmol/min/mg protein in HG3. On the other hand, the imidaprilat formation in HLC ranged from 2.0 pmol/min/mg protein in HH47 to 47.1 pmol/min/mg protein in HG3. The imidaprilat formation between individual HLM and HLC from the same donors was well-correlated ($n = 6$, $r = 0.77$).

Individual Kinetic Analysis of Imidaprilat Formation in HLM and HLC

Kinetic analyses of the imidaprilat formation were performed in some individual HLM and HLC (Tab. 2). The imidaprilat formation in both HLM and HLC with high activities fitted to the Michaelis-Menten equation, whereas those with low activities fitted curved lines in the Eadie-Hofstee plots (Fig. 3). The K_m values in HLM with high activities were higher than the S_{50} values in HLM with low activities.

Kinetic Analysis of Deraprilat Formation in Human Liver, Rat Liver, and Rat Jejunum

To investigate the effects of structural diversity on the kinetic analysis, kinetic analyses of the deraprilat formation were performed in pooled HLM, pooled HLC, RLM, RLC, RJM, and RJC. The kinetic parameters of the deraprilat formation are shown in Table 3. The Eadie-Hofstee plot of the deraprilat formation was bi-phasic in pooled HLM whereas it was curved in pooled HLC. RLM also appeared bi-phasic in the Eadie-Hofstee plot. The V_{max}/K_m values of high and low affinity isoforms in RLM were higher than those in pooled

Table 2. Kinetic Parameters of Imidaprilat Formation in Individual HLM and HLC

Enzyme Source	Activity	Donor	K_m (μM)	V_{max} (pmol/min/mg)	V_{max}/K_m (μL/min/mg)	n	Model
HLM	High	HG3	119	2310	19.4	—	Michaelis-Menten
		HH31	175	1963	11.2	—	
	Low	HH47	15[a]	48	1.7[b]	1.5 (1.5[c])	Hill
		HG64	84[a]	349	2.9[b]	1.1 (1.1[c])	
HLC	High	HH18	444	905	2.0	—	Michaelis-Menten
		HG89	205	305	1.5	—	
	Low	HH47	420[a]	56	0.1[b]	1.0 (1.2[c])	Hill
		HH31	340[a]	124	0.4[b]	1.0 (1.2[c])	

n, Hill coefficient calculated using all concentrations of imidapril.
[a] S_{50}.
[b] CL_{max}.
[c] Hill coefficient calculated below 100 μM imidapril.

DOI 10.1002/jps